AGNs Mass Estimation Using Single-Epoch Virial Method with Empirical Parameters Optimization

Shubham Apte

1 Introduction

Active Galactic Nuclei (AGN) are the highly energetic centers of galaxies, powered by accretion onto a supermassive black hole (SMBH). The immense energy and radiation emitted from these regions, including high-intensity broad emission lines, make AGN critical objects for studying SMBH properties, galaxy evolution, and the role of black holes in galaxy formation. One important parameter of interest is the mass of the SMBH, as it has profound implications for host galaxy evolution.

In the local universe, SMBH masses are estimated by resolving the dynamics of stars or gases. But for distant AGNs, measurements of the virial motion of gas in the broad-line region (BLR) is used. The broad lines imply that the gas must be either extremely hot or in rapid motion. The structure of most of the AGNs consists of a central spherical source emitting radiation, surrounded by a disk shaped clouds of matter & gas called accretion disk. The front portion of the disk facing the source are highly ionized, emitting high-ionization lines such as He II, He I, O VI, N V, and C IV. Whereas due to the thickness of the disk, the posterior portion emits low-ionization lines such as Mg II, Ca II, O I, and Fe II.

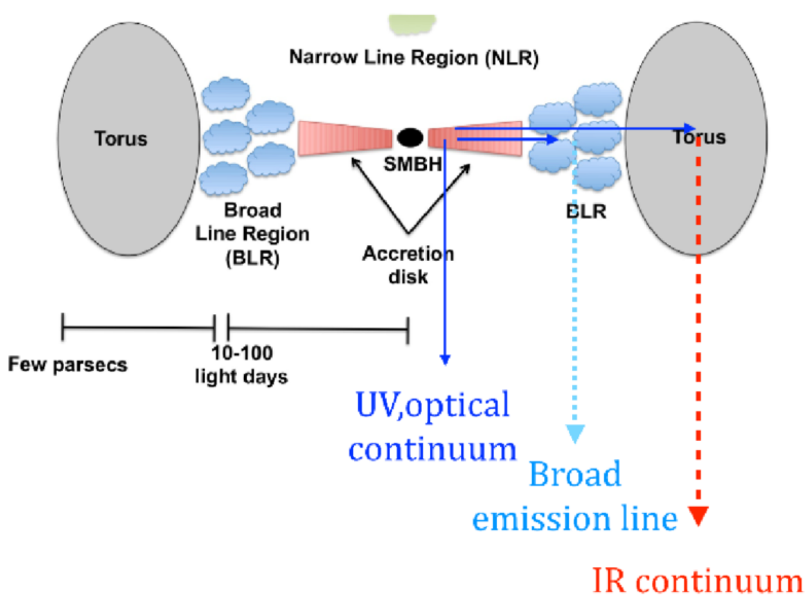

Figure 1: AGN Structure

There are a few widely used approaches for SMBH mass measurement. The most precise method for computing virial masses is reverberation mapping which yields accurate SMBH mass estimates consistent with dynamical masses. Reverberation mapping measures the velocity of clouds in the BLR from the width of broad emission lines and the BLR size from the time lag between the continuum and emission line variability. It requires spectroscopic observations over a large period of time at high cadence, which limits the application of this technique.The only method for estimating SMBH virial masses for a large number of sources is single-epoch spectroscopy , which relies on the tight correlation between quasar continuum luminosity and BLR size to compute SMBH masses from a single spectrum. But these lesser requirements translate into noisier SMBH mass estimates. Generally, for low redshift AGNs, the $H\beta$ line is mostly used as a virial broadening estimator of the SMBH mass [1], whereas for high redshift AGNs C IV and Mg II lines are used [2].

2 Single-Epoch Virial Mass Determination Method

The Virial theorem in provides a relationship between the gravitational potential energy and kinetic energy of a bound system. For AGN, the gas in the BLR is assumed to be gravitationally bound to the SMBH. This assumption allows us to estimate the mass of the SMBH by using motion of BLR gas, by observing the broadening of emission lines like $H\beta$ & Mg II. In this context, the virial theorem implies that:

$$M_{\rm BH} = \frac{R_{\rm BLR}\Delta V^2}{G} \tag{1}$$

where ΔV is the velocity of the BLR gas, G is the gravitational constant, and f is the Virial factor, which is a dimensionless scale factor representing unknown geometry and distribution of BLR. f is not directly measurable for individual AGNs, but the average has been empirically determined [3], while the continuum luminosity can be used to estimate the system size through the $R_{\rm BLR}/L$. Single-epoch mass estimators are expressed as:

$$\log(M_{\rm BH}({\rm RM})/M_\odot) = \alpha + \beta \log L_{\rm continuum} + \gamma \log \Delta V \tag{2}$$

Here $L_{\rm continuum}$ is the continuum luminosity and ΔV is the line width of a broad emission line. Calibrating the above equations, we get:

$$\log M_{\rm BH} = \alpha + \beta \log\left(\frac{L}{10^{44}\,{\rm erg/s}}\right) + \gamma \log\left(\frac{\rm FWHM}{1000\,{\rm km/s}}\right) \tag{3}$$

Here FWHM is the full width at half maximum of a specific emission line & the parameters α, β, γ are empirically determined, having different values across literature (though, value of gamma is taken to be approx 2 everywhere) based on comparison against direct SMBH mass measurements.

In this work, our focus will be on deriving the $\log M_{BH}$ values for various empirical parameters mentioned across literature, & observe the linear fit with the direct SMBH measurements. For this analysis, We will restrict ourselves to the $H\beta$ & MgII lines only. Furthermore, we will optimize their values by the minimization of error technique to best fit the actual values for a given dataset.

3 Data selection

Diverse datasets were collected as to observe the parameter optimization for distinct AGNs. A dataset consisting of optical spectroscopy of 165 flat spectrum radio quasars (FSRQs) in the Fermi 1LAC sample by [4] was selected. Along with this, a sample of 154 type 1 AGN belonging to the XMM-Newton serendipitous sample (XBS) was chosen from [5]. Both the catalogs are available online on CDS. Both the former and latter datasets contained accurate actual SMBH masses, which we used for the error minimization of empirical parameters.

4 Methodology

First, the log$\mathrm{FWHM}_{H\beta}$ was plotted against logFWHM_{MgII} to verify the observations are closely related to each other, and do not show large deviations in both the datasets.

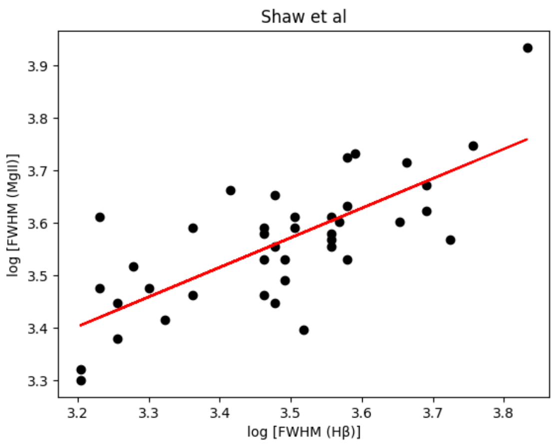

(a) Linear fit [4]

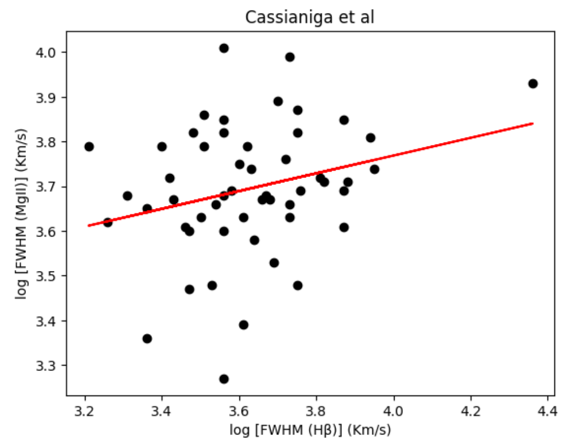

(b) Linear fit for [5]

Figure 2:

After this verification, the M_{BH} values were calculated from log λL_{λ} at 5100 $\mathring{A}$ & 3000 $\mathring{A}$, & the FWHM values for both $H\beta$ & MgII respectively. The α & β values were taken from [6], [7], [4] for $H\beta$ & from [6], [8], [9] for MgII. The maximum error values obtained using the values from these literature were in the range 2 $M_{\odot}$ and the minimum were 0.29 $M_{\odot}$ (see figure 6 & 4).

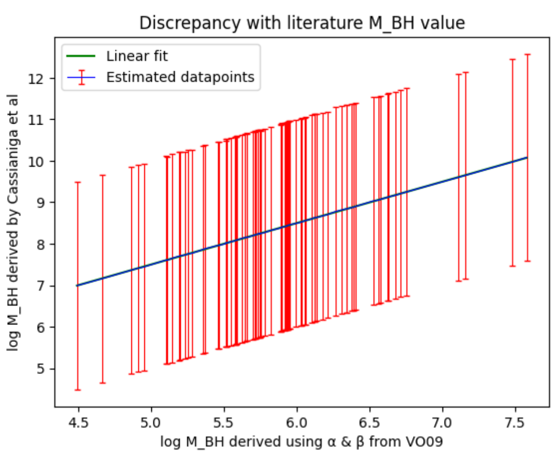

(a) $H\beta$ discrepancy with [5] M_{BH}

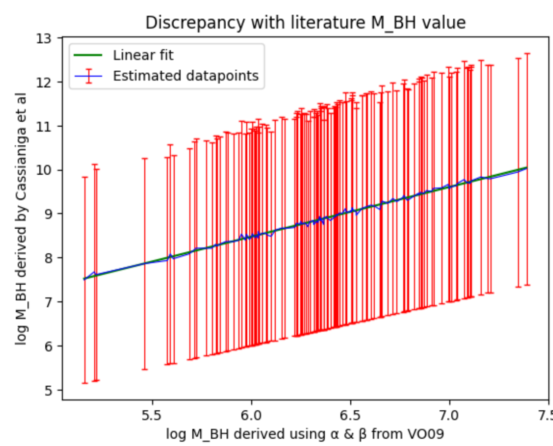

(b) MgII discrepancy with [5] M_{BH}

Figure 3:

5 Optimization of Empirical Parameters

These α & β values needed to be optimized for this particular dataset, as their values derived in above mentioned literature used discrete datasets that of our own. Therefore the discrepancy in the

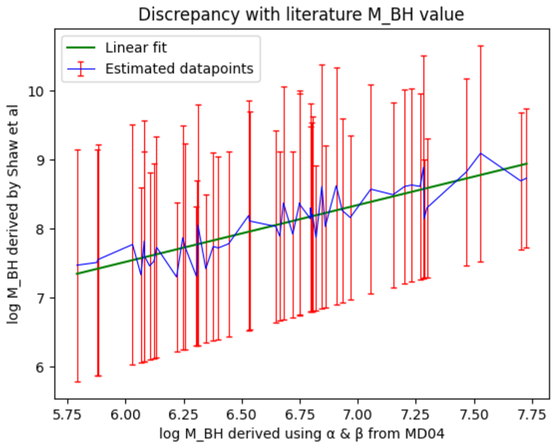

(a) $H\beta$ discrepancy with [4] M_{BH}

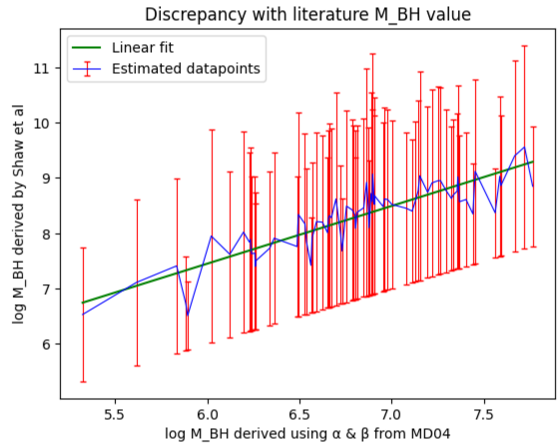

(b) MgII discrepancy with [4] M_{BH}

Figure 4:

parameters was obvious and was observed. To minimize this fluctuation, the optimization objective function was defined as:

$$\text{error}(\alpha, \beta) = \sum (\text{Observed\_Mass} - \text{Calculated\_Mass})^2 \tag{4}$$

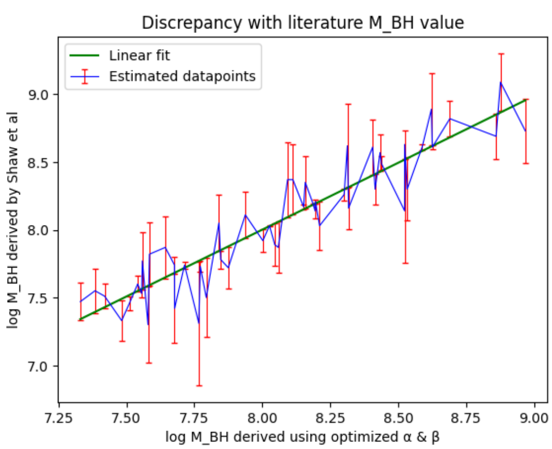

(a) $H\beta$ Optimization fit with [4] M_{BH}

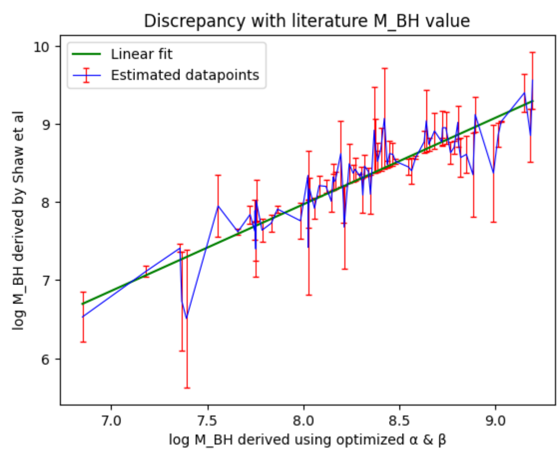

(b) MgII Optimization fit with [4] M_{BH}

Figure 5:

where Calculated_Mass uses the formula with the current α and β values. This process iteratively adjusts α and β to minimize the mean squared error using Nelder-Mead algorithm. The resulting error bar shows a nearly perfect fit with the M_{BH} calculated using re-evaluated optimized empirical parameters.

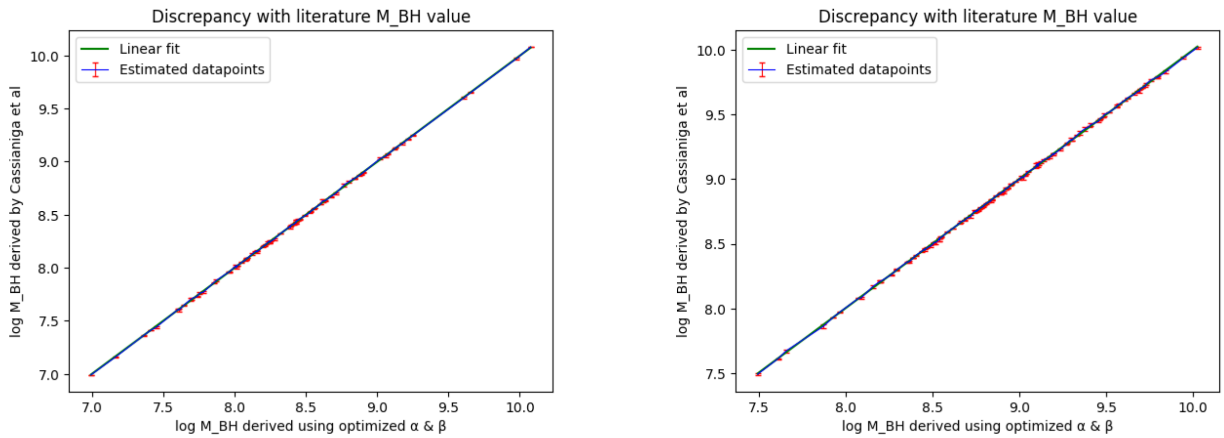

(a) $H\beta$ Optimization fit with [5] $M_{\rm BH}$

(b) MgII Optimization fit with [5] $M_{\rm BH}$

Figure 6:

6 Results of Optimization

The optimization converged successfully, yielding refined values for α and β that minimized the error. These optimized parameters produced SMBH mass estimates with a smaller deviation with [4] values, and negligible deviation with [5] validating the effectiveness of the optimization. The parameter values thus obtained after optimization are stated below:

For $M_{\rm BH}$ estimate using $H\beta$ in [4]:

$$(\alpha, \beta) = (3.1649, 0.47546)$$

For $M_{\rm BH}$ estimate using MgII in [4]:

$$(\alpha, \beta) = (2.379, 0.5737)$$

For $M_{\rm BH}$ estimate using $H\beta$ in [5]:

$$(\alpha, \beta) = (3.4236, 0.4979)$$

For $M_{\rm BH}$ estimate using MgII in [5]:

$$(\alpha, \beta) = (2.4, 0.6199)$$

These values provided improved SMBH mass estimates when compared to observed values in our dataset, demonstrating the value of parameter optimization in reducing residual errors.

7 Conclusion

The single-epoch virial mass determination method, with refined parameters obtained through optimization, offers a viable and accurate approach for estimating SMBH masses in AGN. By using optimization techniques to minimize deviations from observed values, the accuracy of mass predictions was enhanced. This approach can be scaled to larger AGN samples or adapted to other emission lines for broader studies.

References

[1] R. J. McLure and J. S. Dunlop, "The black hole masses of Seyfert galaxies and quasars," , vol. 327, pp. 199–207, Oct. 2001.

[2] N. Rakić, "Kinematics of the H α and H β broad-line region in an SDSS sample of type-1 AGNs," , vol. 516, pp. 1624–1634, Oct. 2022.

[3] C. A. Onken, L. Ferrarese, D. Merritt, B. M. Peterson, R. W. Pogge, M. Vestergaard, and A. Wandel, "Supermassive Black Holes in Active Galactic Nuclei. II. Calibration of the Black Hole Mass-Velocity Dispersion Relationship for Active Galactic Nuclei," , vol. 615, pp. 645–651, Nov. 2004.

[4] M. S. Shaw, R. W. Romani, G. Cotter, S. E. Healey, P. F. Michelson, A. C. S. Readhead, J. L. Richards, W. Max-Moerbeck, O. G. King, and W. J. Potter, "Spectroscopy of broad-line blazars from 1lac," *The Astrophysical Journal*, vol. 748, p. 49, mar 2012.

[5] A. Caccianiga, R. Fanali, P. Severgnini, R. Della Ceca, E. Marchese, and S. Mateos, "Black-hole masses of type 1 AGN in the XMM-Newton bright serendipitous survey," , vol. 549, p. A119, Jan. 2013.

[6] R. J. McLure and J. S. Dunlop, "The cosmological evolution of quasar black hole masses," , vol. 352, pp. 1390–1404, Aug. 2004.

[7] M. Vestergaard and B. M. Peterson, "Determining Central Black Hole Masses in Distant Active Galaxies and Quasars. II. Improved Optical and UV Scaling Relationships," , vol. 641, pp. 689–709, Apr. 2006.

[8] M. Vestergaard and P. S. Osmer, "Mass Functions of the Active Black Holes in Distant Quasars from the Large Bright Quasar Survey, the Bright Quasar Survey, and the Color-selected Sample of the SDSS Fall Equatorial Stripe," , vol. 699, pp. 800–816, July 2009.

[9] Y. Shen, G. T. Richards, M. A. Strauss, P. B. Hall, D. P. Schneider, S. Snedden, D. Bizyaev, H. Brewington, V. Malanushenko, E. Malanushenko, D. Oravetz, K. Pan, and A. Simmons, "A Catalog of Quasar Properties from Sloan Digital Sky Survey Data Release 7," , vol. 194, p. 45, June 2011.